Gain-assisted optical switching in plasmonic nanocavities

Yun Shen (沈 云)[1*], Guoping Yu (于国萍)[2], Jiwu Fu (傅继武)[1], and Liner Zou (邹林儿)[1]

[1]*Department of Physics, Nanchang University, Nanchang 330031, China*

[2]*Key Laboratory of Acoustic and Photonic Materials and Devices, Ministry of Education,*

Department of Physics, Wuhan University, Wuhan 430072, China

[*]Corresponding author: shenyunoptics@gmail.com

A plasmonic cavity filled with active material is proposed to explain optical switching. Optical properties, including transmission, response time, and field distribution of on/off state, are numerically investigated. We demonstrate that such a gain-assisted plasmonic structure can achieve optical switching in the nanodomain and shorten the switching time to the subpicosecond level. Our results indicate the potential application of the proposed structure in optical communication and photonic integrated circuits.

OCIS codes: 130.4815, 240.6680, 140.3945.

doi: 10.3788/COL201210.021301.

Gain-assisted propagation of surface plasmon polaritons (SPPs) has recently attracted increased attention, particularly in perspectives including absorption compensation[1−3], group velocity manipulation[4,5], and lasing spacers[6−10]. Plasmonic cavities filled with active materials were studied by Shen *et al.*[5], who showed that controllable group velocity could be achieved through the dispersion of active materials by tuning gain strength, thus offering a feasible way of obtaining synchronization, time-division multiplexing, and equalization, among others. An important property of gain-assisted plasmonic cavities was discussed: tuned gain strength could lead to varied loss of active material and bring about plasmonic cavities with different transmissions[5]. Tunable transmission has potential applications in constructing optical switching, which is very important for optical communications and has been demonstrated in various structures[11−13]. Intensive studies on gain-assisted plasmonic cavities for optical switching are currently under development. An active material described by the Lorentz model and filled into a metal gap waveguide (MGW) has been proposed, and important optical properties, including transmission and field distributions of the on/off switching state, have been investigated[12,13]. In particular, the response times of optical switching have been comprehensively studied. Finite-domain time-difference (FDTD) and the transfer matrix method have demonstrated that such a gain-assisted plasmonic structure can achieve optical switching in the nanodomain and shorten switching times to the subpicosecond level. Specifically, the switching time determined by the geometry of the structure was shortened to 0.6 ps. These results imply the significant potential applications of gain-assisted plasmonic structures in optical communication and integrated photonics[14,15].

The proposed structure is schematically shown in Fig. 1. A layer of the active material with thickness w and length L is filled into a Ag film-constructed MGW. Here, h_m is the thickness of the metal film, and ε_0 and ε_m denote the dielectric constants of air and metal, respectively. ε_1 is the dielectric constant of the active material and can be demonstrated by the Lorentz model[5,16],

which shows that $\varepsilon_1 = \varepsilon_\infty^1 + A \cdot \omega_1^2/(\omega_1^2 - \omega^2 - j\gamma_1\omega)$, where ε_∞^1, ω_1, and γ_1 are the base-level electric permittivity, resonant frequency, and damping constant, respectively; A is the macroscopic analog of the Lorentz oscillator strength, which can be continuously varied by electrically or optically pumping the active materials. $A > 0$ corresponds to a regime with less than 50% of the population in excited state, manifesting optical loss, and $A < 0$ represents an inverted system, manifesting optical gain. The effective refractive index $n_{\mathrm{eff}i}(\varepsilon_i)(i=0, 1)$ of the MGW can be read as $n_{\mathrm{eff}i}(\varepsilon_i) = \beta_{\mathrm{spp}i}(\omega)/k_0$[17,18], where k_0 is the wave number of light in air, and $\beta_{\mathrm{spp}i}$ is the propagation constant of SPPs in the MGW related to ε_0 and ε_1. While the interfaces between the air and the active material layer in the MGW form two mirrors, the waveguide region, consisting of Ag and ε_1, can function as a plasmonic Fabry-Perot (F-P) cavity. The transmission of the F-P cavity can be calculated by transfer matrix method.

Besides the calculation in Ref. [5], the active material layer in our calculation is set as quantum dots embedded in semiconductors with ultrafast (<200 fs) gain recoveries and $\varepsilon_\infty^1 \approx 11.30$, $\omega_1 = 0.80$ eV (1 550 nm), and $\gamma_1 = 0.02\omega_1$ in the Lorentz model[5,19−21]. The calculated real and imaginary parts of ε_1 for $A = -0.011$ and 0.005 are separately illustrated in Figs. 2(a) and (b). In Fig. 2(b), the negative and positive values of the imaginary part of ε_1, corresponding to $A < 0$ and $A > 0$, manifest optical gain and loss, respectively. Figures 2(c) and (d) respectively show the real and imaginary parts of $n_{\mathrm{eff}1}$ of the MGW composed of Ag and ε_1 with $w=22$ nm, in which Ag is described
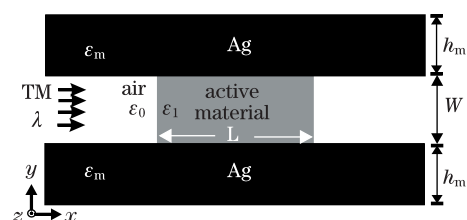

Fig. 1. Scheme of the proposed structure constructed by an active material layer filled into a Ag film-constructed MGW.

by the Drude model $\varepsilon_{\mathrm{m}} = \varepsilon_\infty^m - \omega_p^2/(\omega^2 + \mathrm{j}\gamma_{\mathrm{m}}\omega)$ with $(\varepsilon_\infty^m, \omega_p, \gamma_{\mathrm{m}}) = (1,\ 7.75\ \mathrm{eV},\ 0.08267\ \mathrm{eV})$ in the near-infrared range[22]. In Figs. 2(c) and (d), solid curves and dotted curves correspond to $A=-0.011$ and 0.005, respectively. Figure 2(d) shows that significant differences in SPP loss exist between $A=-0.011$ and 0.005 at around 1 550 nm. The optical gain (solid curves) can obviously compensate losses of the SPP waveguide. Therefore, the tunable loss, dominated by A, leads to probability of on/off state of intensity. Note that the imaginary parts of n_{eff} remain positive for $A=-0.011$, which means that the optical gain is insufficient to completely compensate for SPP losses.

To allow the plasmonic cavity to work around an optical communication wavelength of 1 550 nm, the transmission properties for different values of L with a 1 550-nm incident light and $A=-0.011/0.005$ are first studied. The results obtained by the transfer matrix method are shown in Fig. 3(a). In the calculation, TM-polarized (the magnetic field is parallel to the z axis) light is considered, and magnetic field intensity $|H_z|^2$ at the center of a plane outside the F-P cavity 1 nm (12 nm) away from the front (back) mirror represents the input (output). Figure 3(a) shows that the transmission varies with L and peaks, which correspond to the resonance occurring in the plasmonic cavity, appear at intervals. In Fig. 3(a), the transmission of $A=-0.011$ is obviously higher than that of $A=0.005$ because the former corresponds to smaller SPP losses than the latter at 1 550 nm (see Fig. 2(d)). An important phenomenon in Fig. 3(a) is that a significant difference in the transmission between $A=-0.011$ and 0.005 occurs at around the resonance of the plasmonic cavity. This can be understood by the following analysis. For a given input incidence and transmission coefficient for the back mirror of the plasmonic cavity, the output and transmission are determined by the intensity in the cavity. When it is off-resonant, the intensities in the cavity for $A=-0.011$ and 0.005 are both small, and their difference is insignificant. As resonances occur, the intensities in the cavity for different A are magnified, i.e., the difference is enlarged. For instance, when $L=352$ nm with resonance of cavity, the transmission of the incident signal light (1 550 nm) switches from 0.2805 to 0.9365 as A changes from 0.005 to –0.011, showing significant switching.
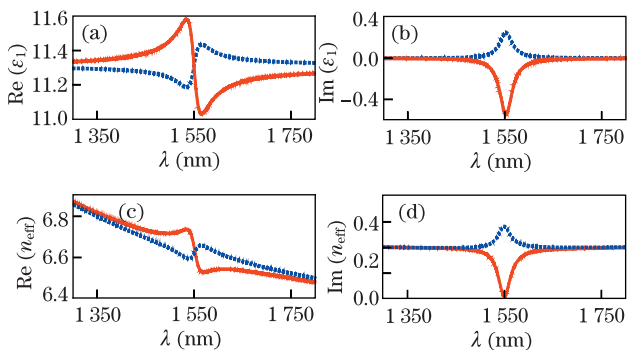

Fig. 2. (a) and (b) Real and imaginary parts of ε_1; (c) and (d) real and imaginary parts of n_{eff1}. Solid curves and dotted curves correspond to $A = -0.011$ and 0.005, respectively.
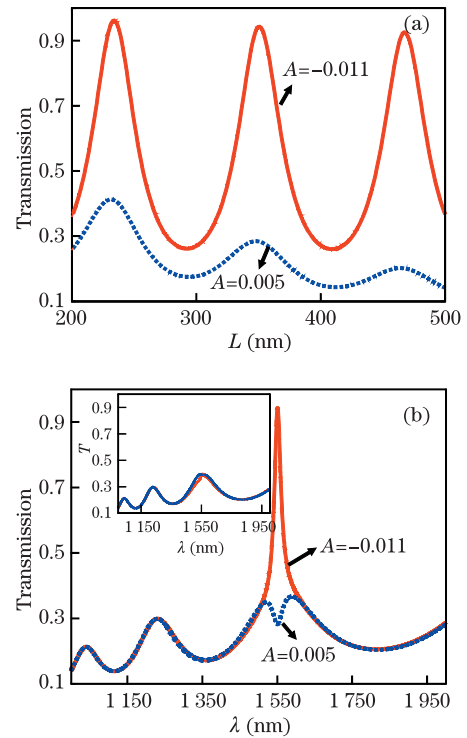

Fig. 3. (a) Dependence of transmission on L for 1 550 nm incidence; (b) dependence of transmission on incident wavelength for $L=352$ nm. The imaginary parts of ε_1 (Fig. 2(b)) are ignored, and the transmission spectra are shown in the inset. Solid curves and dotted curves correspond to $A =-0.011$ and 0.005, respectively.

To obtain a clear understanding of the switching effect, the transmission in different incident wavelengths is illustrated in Fig. 3(b) for $A=-0.011$ and 0.005 with $L=352$ nm given. The inset of Fig. 3(b) shows the transmission as the imaginary parts of ε_1 (Fig. 2(b)) are set to zero. Comparing Fig. 3(b) with the inset, a significant difference in the transmission at 1 550 nm is caused mainly by differences in the imaginary part of ε_1, i.e., the gain/loss of the active material leads to high/low transmission. Although the values of the real parts of ε_1 (Fig. 2(a)) and n_{eff1} (Fig. 2(c)) are different for $A=-0.011$ and 0.005 near 1 550 nm, the transmission (Fig. 3(b) inset) is minimally affected by the difference. In other words, it is the cross-gain, not the cross-phase modulation, of the active material that results in the switching behavior.

The response time is another important quantity for optical switching. Figure 4 shows the response time of a structure with $L=532$ nm at $\lambda=1\,550$ nm, which is calculated using FDTD. In the calculation, a square pulse of A switching between $A=0.005$ and –0.011 (Fig. 4, dotted curve) is launched into the system with a duration of 2 ps by external pumping of the active material. As a result, the transmission switches between 0.9554 and 0.2965 (Fig. 4, solid curve). We can see that the switching time for up and down are 0.6 and 0.4 ps, respectively, which are ultrafast values. Evidently, the switching up time is longer than the switching down time. This is because light in the cavity with smaller losses requires a longer round trip to become stable. Note that the gain recovery time of the active material
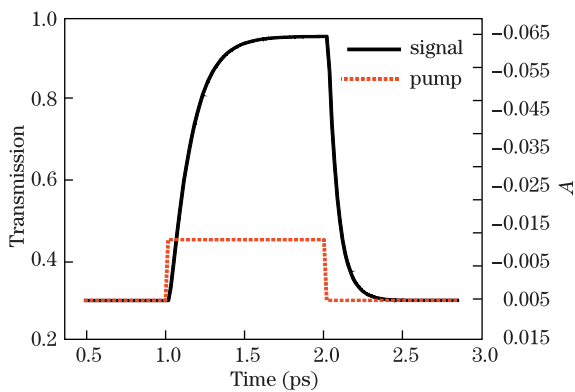
Fig. 4. Gain strength A of the active material (dashed curve) and transmission of incident signal light (solid curve) as functions of time.
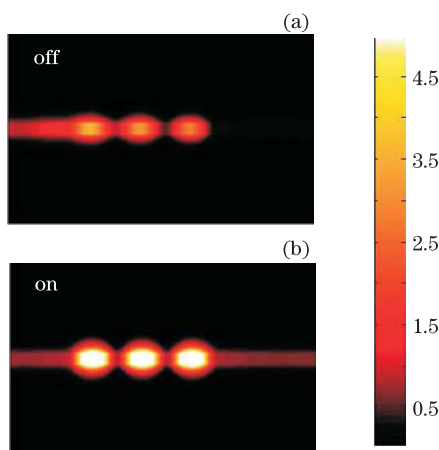

Fig. 5. Magnetic-field $|H_z|^2$ distributions for $A=0.005$ and -0.011 corresponding to (a) off and (b) on states. The signal light is launched from the left side.

is not considered in our calculation; hence the switching time of 0.6 ps is only determined by the feedback of the structure, which represents the shortest switching time of the structure. The final switching time, which is determined by the response time of the geometry of the structure together with the response time of the active material, can be shortened to the subpicosecond level as an ultrafast ($<$200 fs) gain recovery of the active material used in our structure.

To illustrate its switching property, magnetic-field $|H_z|^2$ distributions in the gain-assisted structure for $A=0.005$ and -0.011 corresponding to off and on states are shown in Figs. 5(a) and (b), respectively. For the off state, the light in the plasmonic cavity is weak, and the light behind the cavity is near zero, indicating that the signal light is cut off by the plasmonic cavity. In contrast, the magnetic field for the on state shows large intensity both in and behind the cavity, indicating high transmission.

In conclusion, optical switching of a subwavelength plasmonic cavity containing an active material described by the Lorentz model is numerically investigated. Impor-

tant optical properties of the switching structure, including transmission, response time, and field distribution of the on/off state are studied. The results demonstrate that gain-assisted plasmonic switches can scale the structure size down to the nanodomain and shorten switching up/down times to 0.6/0.4 ps, as determined by the geometry of the structure. These results indicate the potential applications of the structure in optical communication and photonic integrated circuits.

References

1. M. A. Noginov, G. Zhu, M. Bahoura, J. Adegoke, C. E. Small, B. A. Ritzo, V. P. Drachev, and V. M. Shalaev, Opt. Lett. **31,** 3022 (2006).
2. J. Seidel, S. Grafström, and L. Eng, Phys. Rev. Lett. **94,** 177401 (2005).
3. M. A. Noginov, G. Zhu, M. Mayy, B. A. Ritzo, N. Noginova, and V. A. Podolskiy, Phys. Rev. Lett. **101,** 226806 (2008).
4. A. A. Govyadinov and V. A. Podolskiy, Phys. Rev. Lett. **97,** 223902 (2006).
5. Y. Shen and G. P. Wang, Opt. Express **17,** 12807 (2009).
6. D. J. Bergman and M. I. Stockman, Phys. Rev. Lett. **90,** 027402 (2003).
7. M. I. Stockman, Nat. Photon. **2,** 327 (2008).
8. N. I. Zheludev, S. L. Prosvirnin, N. Papasimakis, and V. A. Fedotov, Nat. Photon. **2,** 351 (2008).
9. M. A. Noginov, G. Zhu, A. M. Belgrave, R. Bakker, V. M. Shalaev, E. E. Narimanov, S. Stout, E. Herz, T. Suteewong, and U. Wiesner, Nature **460,** 1110 (2009).
10. M. I. Stockman, J. Optic. **12,** 024004 (2010).
11. H. Wang, D. Goorskey, and M. Xiao, Phys. Rev. Lett. **87,** 073601 (2001).
12. C. Min and G. Veronis, Opt. Express **17,** 10757 (2009).
13. W. Cai, J. S. White, and M. L. Brongersma, Nano Lett. **9,** 4403 (2009).
14. X. Wang, P. Wang, C. Chen, J. Chen, Y. Lu, H. Ming, and Q. Zhan, Chin. Opt. Lett. **8,** 584 (2010).
15. A. E. Willner, L. Zhang, Y. Yue, and X. Wu, Chin. Opt. Lett. **8,** 909 (2010).
16. A. A. Govyadinov, V. A. Podolskiy, and M. A. Noginov, Appl. Phys. Lett. **91,** 191103 (2007).
17. I. P. Kaminow, W. L. Mammel, and H. P. Weber, Appl. Opt. **13,** 396 (1974).
18. Y. Shen and G. P. Wang, Opt. Express **16,** 8421 (2008).
19. S. Schneider, P. Borri, W. Langbein, U. Woggon, R. L. Sellin, D. Ouang, and D. Bimberg, IEEE Photon. Technol. Lett. **17,** 2014 (2005).
20. V. I. Klimov, A. A. Mikhailovsky, S. Xu, A. Malko, J. A. Hollingsworth, C. A. Leatherdale, H. J. Eisler, and M. G. Bawendi, Science **290,** 314 (2000).
21. G. M. Ribeiro, R. L. Maltez, A. A. Bernussi, D. Ugarte, and W. de Carvalho, Jr., J. Appl. Phys. **89,** 6548 (2001).
22. E. D. Palik, *Handbook of Optical Constants of Solids* (Academic, London, 1985).